Available online at www.equijost.com

Equity Journal of Science and Technology, 2023 10(2): 10 - 16

ISSN 2354-1814; E-ISSN 2683-5961

EQUIJOST *An Official Publication of Kebbi State University of Science and Technology, Aliero, Nigeria*

Numerical investigation on the impact of Hole Transporting Layer (HTL) using SCAPS-1D on tin-based perovskite solar cells.

[1]Bello U. Gwandu, [2]Yahaya H. Nawawi, [3]Sani Faruk, [1]Abubakar S. Zauro

[1]Department of Energy and Applied Chemistry, Usmanu Danfodiyo University Sokoto, Nigeria

[2]Department of Electrical and Electronics, Usmanu Danfodiyo University Sokoto, Nigeria

[3]Department of Physics, Usmanu Danfodiyo University Sokoto, Nigeria

*Corresponding Author's email: Umargwandu09@gmail.com

Abstract

Hole transport layers (HTL) are the primary elements of Perovskite solar cells (PSCs), which have can lower losses and nonradiative recombination. It serves a significant function in device performance due to its numerous advantages such as good conductivity, solution processability and suitable energy level that matches the perovskite absorber layer. Therefore, finding more cost-effective and stable HTL for perovskite-based solar cells is essential. The primary goal of this work is to investigate the best alternative HTL in methyl ammonium tin iodide perovskite solar cells and to investigate the influence of different HTL (such as CuI, Cu_2O and SpiroOMeTAD) on the performance of planar structure; FTO/TiO_2/$CH_3NH_3SnI_3$/HTL/Au using Solar capacitance simulator software. To achieve optimal performance, some parameters such as the absorber layer thickness, donor concentration as well as operating temperature were varied and examined. The simulated result demonstrates that the absorber layer's thickness has a significant impact on the device's performance, as thickness increases, the Voc dropped; maximum thickness was reached at 1000nm. In addition, the simulated result suggests that the cell's PCE declined with temperature. However high donor concentration deteriorated the device's performance. Among the three selected HTLs, the best performance was obtained with Cu_2O with Voc, Jsc, FF, and PCE of 0.963 V, 32.999 mA/cm2, 80.20%, and 25.48%, respectively. This numerical study shows the potential of producing efficient, cost-effective and stable tin-based perovskite solar cells using inorganic HTL.

Keywords: Hole transporting layer, Flourine doped tin oxide, Power conversion efficiency and SCAPS.

1. Introduction

One way to solve the problems of finding a clean, renewable energy source for our civilization is solar photovoltaics. Perovskite solar cells (PSCs) have lately surfaced as one of the potential choices for an inexpensive and highly efficient solar cell among Si-based solar cells, dye-sensitized solar cells, and organic solar cells [1,2]. These solar cells' light-harvesting layer is made of perovskites, which are materials that can be processed in a solution and also show characteristics of optoelectronic materials that have been researched in solid-state physics [3]. Because of this erratic coalescence, solar photovoltaics may now be processed at room temperature and work with Si-based solar cells [4]. Compared to 3.9% in 2009, power conversion efficiency (PCE) has grown after the perovskite solar cell (PSC) was introduced. Lead-based PSC performance saw a notable 25.8% rise [5]. PSCs are good, but they still require a lot of work to overcome issues of low durability, instability from heat and humidity, and lack of homogeneity. [6,7].

The physical characteristics of the materials, including light collectors (perovskites), contacts, electron and hole transport layers (ETLs), and the device structure, all affect the PCE of PSCs [8]. The primary constituents of PSCs are hole transport layers (HTL), which have the ability to lower nonradiative recombination and losses. [9-11]. Its many benefits, including high conductivity, solution processability, and an appropriate energy level that complements the perovskite absorber layer, have a major impact on a device's performance. For HTL to perform this function of transporting holes to back contact, it must possess a valence band edge situated above the perovskite active layer's valence band edge. Recently, studies have indicated that inorganic HTL are reported with longer stability and high hole mobility than organic HTL [12-14]. Hence, the search for less expensive and more stable HTL for perovskite-based solar cells is imperative. This work's primary goal is to further explore a best alternative HTL in methyl ammonium tin-iodide perovskite solar cells: a computational model to explore the impact of different HTL (such as CuI, Cu_2O, and SpiroOMeTAD) on the performance of the device in planar structure;

FTO/TiO2/CH3NH3SnI3/HTL/ Au using SCAPS [15]. Furthermore, effect of HTL and absorber layer thickness were varied, studied and discussed. Figure1.1 depicts the schematic arrangement of the PSC.

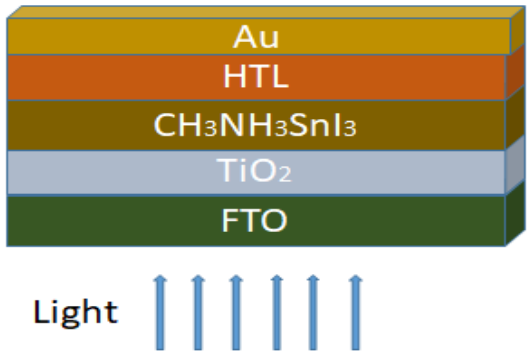

Figure 1.1: Structure of the PSC

2. Materials and method

2.1. Materials

The substances utilized were FTO and Au as front contact and back contact respectively. Hole Transporting materials that include SPIRO-OMETAD, Cu_2O, CuI, TiO_2 was acted as Electron Transporting Layer while $CH_3NH_3SnI_3$ as an Absorber layer. Solar Capacitance Simulator Software (SCAPS) 3.3.10 version

2.2 Method

A planar structure; FTO/TiO2/CH3NH3SnI3/HTL/Au was adopted for this work. The simulation input parameters for the proposed device design were taken from earlier experimental and theoretical literature [16 - 22] hence they were tabulated in Tables 2.1.

Under AM1.5G solar illumination, the numerical simulation in this study was carried out using SCAPS (SCAPS 3.3.10 version) software using the input parameters specified in Table 2.2, an incident power density of 1000 W/cm2, temperature 300 K, work point bias 0 V, frequency of 1.0 X 106Hz, and work point bias 0 V. The Department of Electronics and Information Systems (ELIS) at the University of Gent in Belgium developed the one-dimensional solar cell modeling tool SCAPS [23]. The Poisson equations, the continuity equations for electrons and holes, and the carrier transport equations are the essential semiconductor equations that must be solved in order to get the J-V properties [24]. Figure 2.1 depicts the step-by-step process of the simulation.

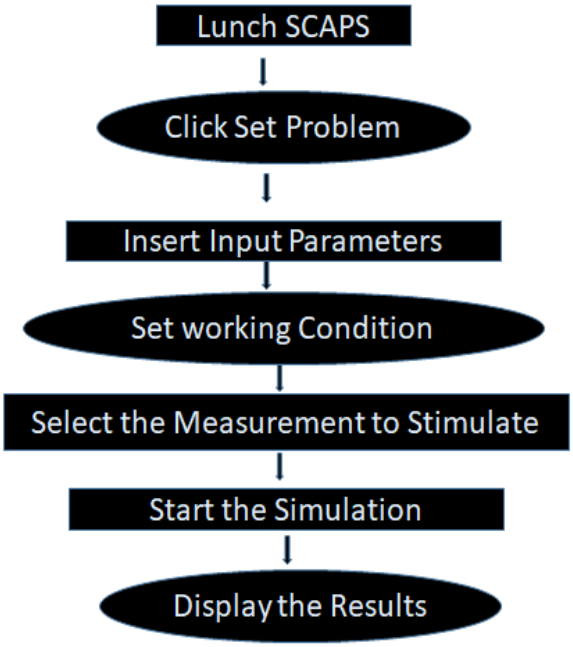

Figure.2.1: step by step procedure in running SCAPS

Table 2.1: Simulation parameters used for the $CH_3NH_3SnI_3$ PSC

Parameters	**FTO**	**TiO2 (ETM)**	**$CH_3NH_3SnI_3$**
Thickness (nm)	300	300	100-500
Bandgap (eV)	3.5	3	1.3
Electron affinity (eV)	4	4	4.17
Dielectric permittivity (relative), εr	9	9	8.2
Conduction band effective density of state ($1/cm^3$)	2.200E+18	2.200E+18	1.0x10E+18
Valence band effective density of state ($1/cm^3$)	1.800E+19	1.900E+19	1.0x10E+18
Electron thermal velocity (cm/s)	1.000E+7	1.000E+7	1.000E+7
Hole thermal velocity (cm/s)	1.000E+7	1.000E+7	1.000E+7
Electron mobility ($cm^2/V.s$)	20	2	1.6
Hole mobility ($cm^2/V.s$)	10	1	1.6
Donor concentration ND ($1/cm^3$)	1.000E+18	1.000E+18	0
Acceptor concentration NA ($1/cm^3$)	0	0	1.0E10+16
Defect density Nt ($1/cm^3$)	1.000E+15	1.000E+15	1.00E+15

Table 2.2: Parameters used for various HTLs

Parameters	SPIRO-OMETAD (HTM)	Cu2O (HTM)	CuI (HTM)
Thickness (nm)	300	300	300
Bandgap (eV)	3.170	2.1	3.1
Electron affinity (eV)	2.050	3.2	2.1
Dielectric permittivity (relative), εr	3	7.11	6.5
Conduction band effective density of state ($1/cm^3$)	2.200E+18	2.200E+18	2.500E+20
Valence band effective density of state ($1/cm^3$)	1.800E+19	1.900E+19	2.500E+20
Electron thermal velocity (cm/s)	1.000E+7	1.000E+7	1.000E+7
Hole thermal velocity (cm/s)	1.000E+7	1.000E+7	1.000E+7
Electron mobility ($cm^2/V.s$)	2.0x10-4	3.4	44
Hole mobility ($cm^2/V.s$)	2.0x10-4	3.4	44
Donor concentration ND ($1/cm^3$)	0	0	0
Acceptor concentration NA ($1/cm^3$)	1.0x10-4	1.000E+18	3.000E+18
Defect density Nt ($1/cm^3$)	1.000E+15	1.000E+15	1.000E+15

3. Results and discussion

3.1 Impact of HTLs on Device Performance

HTL is one of the crucial components of perovskite solar cells. It is essential to the device's effectiveness through is to removed and moved the holes that perovskite absorber layer creates to the back contact (usually Au or Ag). Figure 3.1 displayed the J-V curves of the PSCs with the three different HTLs. Furthermore, Table 3.1 tabulated the PV parameters obtained. It could be seen from Table 3.1 that the device architecture with Cu_2O achieves the highest power conversion efficiency. The best performance was achieved using Cu_2O with V_{oc}, J_{sc}, FF, and PCE of 0.963 V, 32.999 mA/cm^2, 80.20% and 25.48% accordingly. Moreover, the PCE attained by Cu_2O is higher than the PCE attained by Spiro-OMeTAD as reported by [25]. This achievement resulted from the good properties of Cu_2O such as low cost, non-toxicity, small band-gap, and high hole mobility [26].

Table 3.1: Photovoltaic parameters obtained using Spiro-OMeTAD, Cu_2O, and CuI as HTLs

Parameters	Spiro-ometad	Cu_2O	CuI
V_{oc} (V)	0.977	0.963	0.973
J_{sc} (mA/cm^2)	32.367	32.999	31.971
FF (%)	80.040	80.201	75.742
PCE (%)	25.325	25.481	23.571

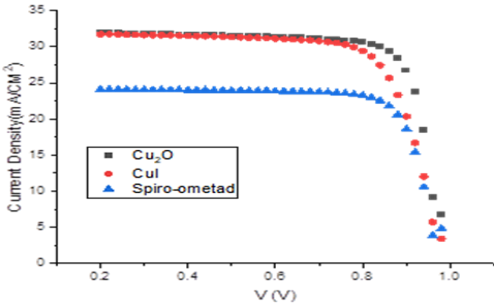

Figure 3.1: Effect of different HTLs on J-V characteristic curve

3.2 Effect of absorber layer thickness of the device using different HTLs

Impact of absorber layer thickness on the device performance in different architectures with several HTL were numerically investigated. While maintaining constant values for the other input parameters, the thickness of the $CH_3NH_3SnI_3$ was changed from 200 nm to 1000 nm, see Figures 3.2 (a – c). The obtained PV parameters were listed in Tables 3.2(a–c). The results show that the V_{oc} decrease given the rise in the absorber layer thickness. According to [27], this is brought on by an increase in charge carrier recombination as the thickness of the absorber layer rises. Furthermore, the results indicate rapid increase in J_{sc} with the increasing absorber layer. This significant increase in J_{sc} results from rise in the production of electron-hole pairs by the light collector and consequently led to increment in the PCE.

Table 3.2 (a): Influence of absorber layer thickness with Spiro-OMeTAD as HTL

Thickness (nm)	V_{oc} (V)	J_{sc} (mA/cm^2)	FF (%)	PCE (%)
200	0.993	24.617	81.603	19.965
400	0.982	31.069	80.736	24.629
600	0.974	33.089	79.386	25.591
800	0.971	33.652	78.302	25.587
1000	0.967	33.729	77.723	25.367

Table 3.2(b): Influence of absorber layer thickness with Cu_2O as HTL

Thickness (nm)	V_{oc} (V)	J_{sc} mA/cm^2)	FF (%)	PCE (%)
200	0.985	25.295	80.458	20.063
400	0.975	31.147	80.959	24.607
600	0.969	32.642	81.123	25.684
800	0.966	33.178	81.010	25.981
1000	0.965	33.393	80.901	26.067

Table 3.2(c): Influence of absorber layer thickness with CuI as HTL

Thickness (nm)	V_{oc} (V)	J_{sc} mA/cm^2)	FF (%)	PCE (%)
200	0.989	24.621	76.086	18.538
400	0.976	31.039	75.456	22.878
600	0.970	32.507	75.815	23.919
800	0.966	33.049	75.666	24.182
1000	0.966	33.277	75.401	24.242

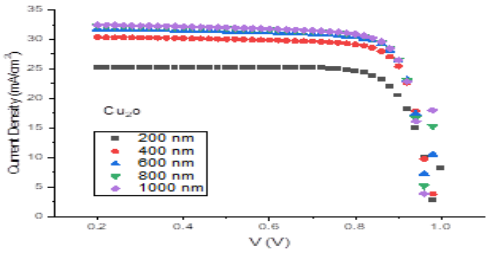

(a)

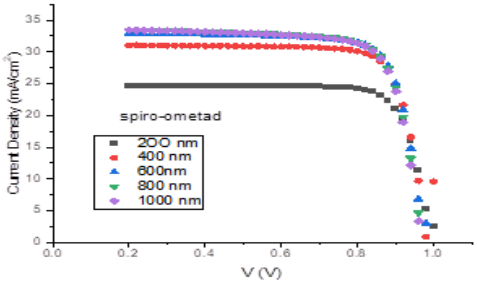

(b)

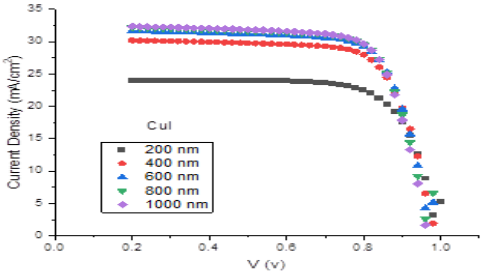

(c)

Figure 3.2: The plotted J-V characteristic curves of the devices with different HTLs

3.3 Impact of Absorber layer Donor concentration using different HTLs

The remaining input parameters remained unchanged while the donor density was changed from 10^{14} cm^{-3} to 10^{20} cm^{-3}. Figures 3.3(a – b) present the plotted J-V curves for CuI, Spiro-OMeTAD Cu_2O, and CuI. In addition, the parameters obtained for Spiro-OMeTAD, Cu_2O, and CuI were similarly displayed in Tables 3.3(a-c). It could be seen from Table 3.3(a), the values for FF were largely dropped leading to significant decrease in PCE. The possible reason for that is the absorber layer accepting majority carriers as reported by [27]. From Table 3.3(b) and (c), no values were recorded for V_{oc} and FF using Cu_2O and CuI. This might be due to interface layer mismatched.

Table 3.3(a): PV parameters for Spiro-OMeTAD with different donor density

Donor Conc.(cm^{-3})	V_{oc} (V)	J_{sc} mA/cm^2)	FF (%)	PCE (%)
10^{14}	0.979	32.370	80.038	25.323
10^{16}	0.944	32.432	78.248	23.965
10^{18}	1.453	24.837	63.270	22.839
10^{20}	4.422	24.094	20.745	22.105

Table 3.3(b): PV parameters for Cu_2O with different donor density

Donor Conc.(cm^{-3})	V_{oc} (V)	J_{sc} mA/cm^2)	FF (%)	PCE (%)
10^{14}	0.972	32.105	81.086	25.311
10^{16}	0.948	32.461	76.859	23.657
10^{18}	2.387	26.299	40.149	25.209
10^{20}	0.000	25.699	0.000	25.685

Table 3.3(c): PV Parameters for CuI with different donor density

Donor Conc. (cm^{-3})	V_{oc} (V)	J_{sc} mA/cm^2)	FF (%)	PCE (%)
10^{14}	0.973	31.980	75.712	25.559
10^{16}	0.952	32.417	67.428	20.822
10^{18}	0.953	32.421	67.430	20.823
10^{20}	0.000	25.663	0.000	25.645

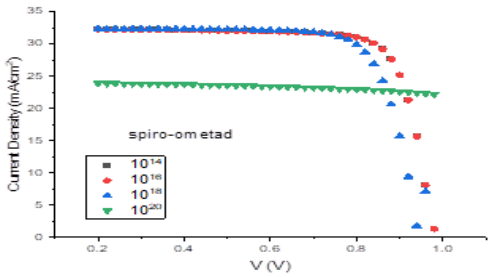

(a)

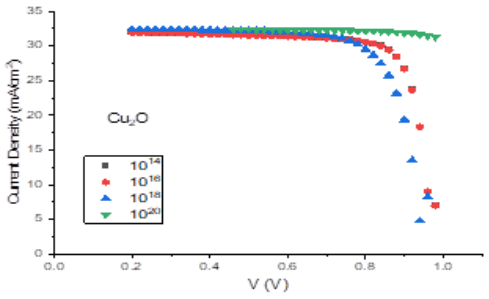

(b)

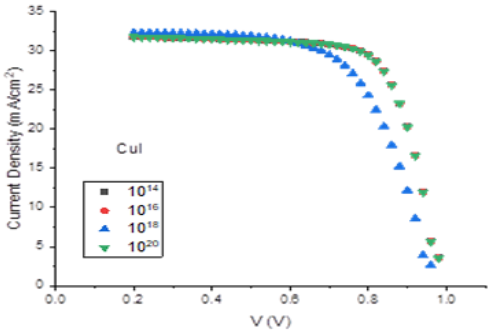

(c)

Figure 3.3: Impact of light absorber donor density on J-V curves

3.4 Effect of Absorber layer operating Temperature using different HTLs

Three distinct HTLs were used to investigate the effects of operating temperature changes on device performance. Specifically, the operating temperature was changed from 300 K to 500 K while maintaining constant input values. The J-V characteristics of the Spiro-OmeTAD, Cu_2O, and CuI-based perovskite solar cells were displayed in Figures 3.4 (a – c) while Tables 3.4 (a - c) contain the obtained parameters. The Tables show that when the operational temperature rises, power conversion efficiency rapidly fall. This could be the result of a drop in V_{oc} brought about by an increase in operating temperature. It is evident that J_{SC} has not undergone any major modifications. This demonstrates that J_{SC} is temperature-independent. In general, the performance of the cell is greatly influenced by the operating temperature. Variations in temperature affects the diffusion length and series resistance, which in turn affects the device's performance [27].

Table 3.4(a): Temperature's impact on the functionality of the device using Spiro-OMeTAD as HTL

Temp. (K)	V_{oc} (V)	J_{sc} mA/cm^2)	FF (%)	PCE (%)
300	0.977	32.367	80.036	25.325
350	0.906	32.371	77.849	22.844
400	0.833	32.371	75.231	20.287
450	0.757	32.379	72.159	17.698
500	0.680	32.432	68.520	15.113

Table 3.4(b): Temperature's impact on the functionality of the device using Cu_2O as HTL

Temp. (K)	V_{oc} (V)	J_{sc} mA/cm^2)	FF (%)	PCE (%)
300	0.972	32.097	81.095	25.312
350	0.899	32.200	79.118	22.917
400	0.824	32.277	77.020	20.489
450	0.747	32.328	74.444	17.987
500	0.669	32.396	71.157	15.433

Table 3.4(c): Temperature's impact on the functionality of the device using CuI as HTL

Temp. (K)	V_{oc} (V)	J_{sc} mA/cm^2)	FF (%)	PCE (%)
300	0.973	31.971	75.744	23.568
350	0.900	31.972	75.696	21.794
400	0.824	31.952	74.393	19.604
450	0.746	31.931	71.913	17.143
500	0.666	31.959	68.504	14.587

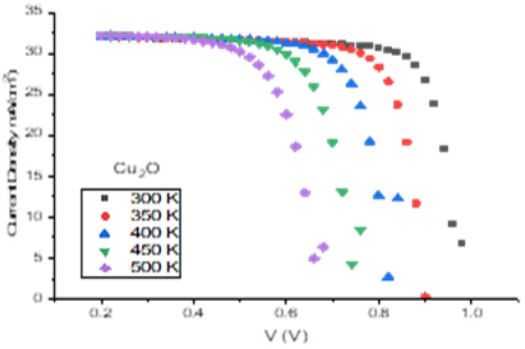

(a)

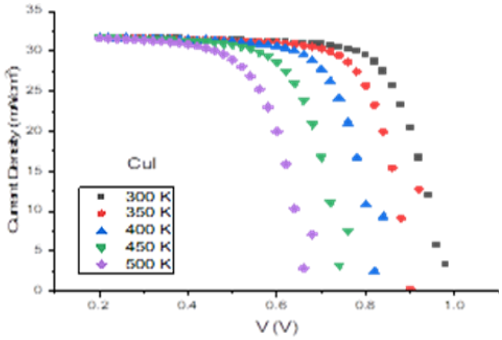

(b)

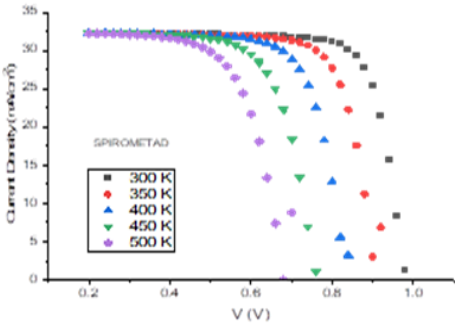

(c)

Figure 3.4: Impact of HTLs temperature on the device performance

4. Conclusions

In this study, a perovskite solar cell free of lead in planar arrangement was designed and modeled using the simulation software SCAPS-1D. Thicknesses of the absorber layer ($CH_3NH_3SnI_3$) were adjusted in order to examine the impact on the photovoltaic characteristics. Our findings demonstrated that absorber layer's thickness has a significant impact on the device's performance; as thickness grows, V_{oc} is seen to drop, with an optimal thickness of 1000 nm The simulated result also demonstrate how the cell's PCE declined with temperature. However, the results revealed that high donor concentration deteriorated the device performance. Among the three selected HTLs, the best performance was obtained with Cu_2O with V_{oc}, J_{sc}, FF, and PCE of 0.963 V, 32.999 mA/cm^2, 80.20%, and 25.48%, accordingly. Therefore, the high performance of Cu_2O could be due to its properties such as band gap (2.17 eV), electron affinity (3.2 eV), hole mobility (80 cms-1) and thickness of 500 nm. Overall, this numerical investigation explores the potential of fabricating affordable, stable, and effective perovskite solar cells made of tin with inorganic HTL.

Acknowledgements
Sincere gratitude is extended to professor Marc Burgelman and his colleagues at University of Gent for granting SCAPS access.

References

1. Liu M, Johnston MB, Snaith HJ. Efficient planar heterojunction perovskite solar cells by vapour deposition. *Nature*. 2013;501(7467):395-8.
2. Green MA, Ho-Baillie A, Snaith HJ. The emergence of perovskite solar cells. *Nature photonics.* 2014; 8(7):506-14.
3. Tai Q, Tang KC, Yan F. Recent progress of inorganic perovskite solar cells. *Energy & Environmental Science.* 2019;12(8):2375-405.
4. Kojima A, Teshima K, Shirai Y, Miyasaka T. Organometal halide perovskites as visible-light sensitizers for photovoltaic cells. *Journal of the American Chemical Society.* 2009;131(17):6050-1.
5. Min H, Lee DY, Kim J, Kim G, Lee KS, Kim J, Paik MJ, Kim YK, Kim KS, Kim MG, Shin TJ. Perovskite solar cells with atomically coherent interlayers on SnO2 electrodes. *Nature*. 2021;598(7881):444-50.
6. Liu WW, Wu TH, Liu MC, Niu WJ, Chueh YL. Recent challenges in perovskite solar cells toward enhanced stability, less toxicity, and large-area mass production. *Advanced Materials Interfaces*. 2019; 6(9):1801758.
7. Berhe TA, Su WN, Chen CH, Pan CJ, Cheng JH, Chen HM, Tsai MC, Chen LY, Dubale AA, Hwang BJ. Organometal halide perovskite solar cells: degradation and stability. *Energy & Environmental Science.* 2016; 9(2):323-56.
8. Courtier NE, Cave JM, Foster JM, Walker AB, Richardson G. How transport layer properties affect perovskite solar cell performance: insights from a coupled charge transport/ion migration model. *Energy & Environmental Science.* 2019;12(1):396-409.
9. Pisoni S, Stolterfoht M, Löckinger J, Moser T, Jiang Y, Caprioglio P, Neher D, Buecheler S, Tiwari AN. On the origin of open-circuit voltage losses in flexible nip perovskite solar cells. *Science And Technology of Advanced Materials*. 2019;20(1):786-95.
10. Ravishankar S, Gharibzadeh S, Roldán-Carmona C, Grancini G, Lee Y, Ralaiarisoa M, Asiri AM, Koch N, Bisquert J, Nazeeruddin MK. Influence of charge transport layers on open-circuit voltage and hysteresis in perovskite solar cells. *Joule*. 2018;2(4):788-98.
11. Liang J, Liu J, Jin Z. All-inorganic halide perovskites for optoelectronics: progress and prospects. *Solar Rrl.* 2017;1(10):1700086.
12. Yang TC, Fiala P, Jeangros Q, Ballif C. High-bandgap perovskite materials for multijunction solar cells. *Joule*. 2018;2(8):1421-36.
13. Yang TC, Fiala P, Jeangros Q, Ballif C. High-bandgap perovskite materials for multijunction solar cells. *Joule*. 2018;2(8):1421-36.
14. Patel PK. Device simulation of highly efficient eco-friendly CH3NH3SnI3 perovskite solar cell. *Scientific Reports*. 2021;11(1):3082.
15. Chen H, Xiang S, Li W, Liu H, Zhu L, Yang S. Inorganic perovskite solar cells: a rapidly growing field. *Solar Rrl*. 2018;2(2):1700188.
16. Patel PK. Device simulation of highly efficient eco-friendly CH3NH3SnI3 perovskite solar cell. *Scientific Reports.* 2021;11(1):3082.
17. Baig F, Khattak YH, Mari B, Beg S, Ahmed A, Khan K. Efficiency enhancement of CH 3 NH 3 SnI 3 solar cells by device modeling. *Journal of Electronic Materials*. 2018; 47:5275-82.
18. Azri F, Meftah A, Sengouga N, Meftah A. Electron and hole transport layers optimization by numerical simulation of a perovskite solar cell. *Solar energy*. 2019; 181:372-8.
19. Minemoto T, Murata M. Impact of work function of back contact of perovskite solar cells without hole transport material analyzed by device simulation. *Current Applied Physics.* 2014;14(11):1428-33.

20. Slami A, Bouchaour M, Merad L. Comparative study of modelling of Perovskite solar cell with different HTM layers. *International Journal of Materials.* 2020; 7:2313-10555.
21. Gan Y, Bi X, Liu Y, Qin B, Li Q, Jiang Q, Mo P. Numerical investigation energy conversion performance of tin-based perovskite solar cells using cell capacitance simulator. *Energies*. 2020;13(22):5907.
22. Burgelman M, Decock K, Niemegeers A, Verschraegen J, Degrave S. SCAPS Manual, department of electronics and information system (elis), university of gent. Belgium; 2016.
23. Movla H. Optimization of the CIGS based thin film solar cells: Numerical simulation and analysis. *Optics*. 2014;125(1):67-70.
24. Gan Y, Bi X, Liu Y, Qin B, Li Q, Jiang Q, Mo P. Numerical investigation energy conversion performance of tin-based perovskite solar cells using cell capacitance simulator. *Energies.* 2020;13(22):5907.
25. Wang Y, Xia Z, Liang J, Wang X, Liu Y, Liu C, Zhang S, Zhou H. Towards printed perovskite solar cells with cuprous oxide hole transporting layers: a theoretical design. *Semiconductor Science and Technology*. 2015;30(5):054004.
26. Bag A, Radhakrishnan R, Nekovei R, Jeyakumar R. Effect of absorber layer, hole transport layer thicknesses, and its doping density on the performance of perovskite solar cells by device simulation. *Solar Energy*. 2020; 196:177-82.
27. Mandadapu U, Vedanayakam SV, Thyagarajan K. Numerical simulation of Ch3Nh3PbI3-XClx perovskite solar cell using SCAPS-1D. *International Journal of Engineering & Scientific Invention.* 2017; 2:40-5.